

Article

Not peer-reviewed version

---

# Multi-Layered Bipolar Ionic Diode Working in Broad Range Ion Concentration

---

[Jaehyun Kim](#) , [Cong Wang](#) , [Jungyul Park](#) \*

Posted Date: 25 May 2023

doi: 10.20944/preprints202305.1706.v1

Keywords: Ion current rectification; Multi-layer; Bipolar ionic diode; Nanochannel network membrane; Nanoparticle



Preprints.org is a free multidiscipline platform providing preprint service that is dedicated to making early versions of research outputs permanently available and citable. Preprints posted at Preprints.org appear in Web of Science, Crossref, Google Scholar, Scilit, Europe PMC.

Copyright: This is an open access article distributed under the Creative Commons Attribution License which permits unrestricted use, distribution, and reproduction in any medium, provided the original work is properly cited.

## Article

# Multi-Layered Bipolar Ionic Diode Working in Broad Range Ion Concentration

Jaehyun Kim <sup>1</sup>, Cong Wang <sup>2</sup> and Jungyul Park <sup>1,\*</sup>

1. Department of Mechanical Engineering, Sogang University, Sinsu-dong, Mapo-gu, Seoul 121-742, Korea; ssamdolr@naver.com

2. School of Mechanical Engineering and Electronic Information, China University of Geosciences (Wuhan), 388, Lumo Road, Wuhan 430074, China; congwang@cug.edu.cn

\* Correspondence: sortpark@sogang.ac.kr; Tel.: +82-2-705-8642

**Abstract:** Ion current rectification (ICR) is the ratio of ion current by forward bias to by backward bias and is a critical indicator of diode performance. In previous studies, many attempts have been continued to improve the performance of this ICR, but there is the intrinsic problem for geometric changes that induce ionic rectification due to their fabrication problem. Additionally, the high ICR could be achieved in the narrow salt concentration range only. Here, we propose a multi-layered bipolar ionic diode based on an asymmetric nanochannel network membrane (NCNM), which is realized by soft lithography and self-assembly of homogenous-sized nanoparticles. Owing to the freely changeable geometry based on soft lithography, the ICR performance can be explored according to the variation of microchannel shape. Interestingly, very stable ICR performance can be achieved using the multi-layered 3D configuration for the bipolar diode in a broad range of salt concentrations (0.1mM ~ 100 mM). This demonstrates the promising potential of multi-layered NCNM for applications in highly concentrated electrolytes, such as biosensors, desalination, or energy harvesting.

**Keywords:** Ion current rectification; Multi-layer; Bipolar ionic diode; Nanochannel network membrane; Nanoparticle

## 1. Introduction

Selective permeation of ions in cell membranes, like the conduction of nerve impulse, play an important role in human activities. Research using artificial nano-channels has been extensively conducted, which mimics the ion-selective permeation of these cells. Artificial nano-channels are more sturdy and reliable than biological nanochannels and can be applied as reverse electrodialysis [1–3] energy harvesting [4–6], ionic memristors [7–9], etc. By introducing asymmetric properties to the nanochannel, the first nanofluid diode device was proposed by Chang et al. [10]. As the EDL in the conical nanopipette overlaps strongly toward the tip, it has high ion selectivity and counter-ions with opposite charge characteristics to the surface of the nanopipette pass smoothly. Therefore, ionic current flows from base to tip under the forward bias and is inhibited under the backward bias. Following this work, various ionic diodes have been studied. Generally, nanofluid diodes can be divided into unipolar and bipolar diodes, depending on whether the polarity of the surface of the nanochannel is unipolar or bipolar [11]. Typical, ion current rectification (ICR), which is critical in the performance, of bipolar ionic diodes better than one of the unipolar diodes. Asymmetric properties of ionic diodes are made of ion tract etching [12–14], anodizing [15,16], etc., and their shapes are conical [17–19], bullet-shaped [18], hourglass [20,21], dumbbell [22], funnel-shaped [23,24] and cylindrical [25], which requires the specialized equipment and expensive fabrication process. Compared to these studies, the nanochannel network membrane (NCNM) made of self-assembled nanoparticles with uniform size can adjust the asymmetric ion transport by changing the geometry of the microchannel through a soft lithography process that is fast, cheap, and easy. The ion selectivity

of the NCNMs is caused by the similar scale of the nanopores from the assembled nanoparticles when compared to the electrical double layer (EDL) [26]. By controlling the size of nanopores, the thickness of EDL that affects the ion distributions can be tunable. The surface charge density and polarity can be controllable by selecting the proper materials for nanoparticles. In the case of NCNM, it is possible to generate ionic concentration gradients along the bias direction and to provoke a rectification phenomenon of ions by providing asymmetric microchannels. In the previous study [27], we conducted the optimization for the parameters contributing to the performances in the single-layered bipolar ionic diode based on NCNM: nanoparticle size, the geometry of NCNMs, and concentration of electrolyte. By thorough investigation of these parameters, a high-rectification ratio was successfully achieved. However, this high performance was possible in only moderately low-concentrated electrolytes (1-10 mM). The ICR was degraded sharply in a very low (0.1mM) or high (>100mM) concentrated environment. Here, we propose a multi-layered bipolar ionic diode with different heights of each NCNM region, which is expected to secure the high-rectification ratio and maintain performance in the broad range of salt concentrations. The rectification characteristics and performance are investigated experimentally according to the variation of geometry in multi-layered microchannel and electrolyte concentration. Following, numerical simulation at 1, 10, and 100mM for single and multi-layered are conducted and compared to support the experimental results.

## 2. Materials and Methods

### 2.1. Fabrication process for multi-layered bipolar ionic diode

Microchannels for a multi-layered bipolar ionic diode were fabricated by a soft-lithography process method. (Figure 1A). The negative photoresist was applied to the silicon wafer (PR, SU-8 2005; Microchem Co., USA) by using spin coater and then soft-baked. Using the mask aligner equipment, the PR on silicon wafer was exposed to UV to make a pattern, and the wafer was hard-baked. And by removing the unexposed PR, a pattern of 5  $\mu\text{m}$  height was formed. Following, a channel height 25 $\mu\text{m}$  and a deep channel height 100 $\mu\text{m}$  were fabricated by using negative photoresist: SU8-2005 and SU8-3050 (Microchem Co., USA) respectively, with the same process in the above. When the master mold is complete, the surface was treated with (3,3,3-trifluoropropyl)silane (452807; Sigma-Aldrich, USA). And then, polydimethylsiloxane (PDMS; Sylgard; Dow Corning Korea Ltd., Korea) was poured over the master mold and heated 95  $^{\circ}\text{C}$  for 1 h on hot plate. Punch out the reservoir of the PDMS device with a 1.5mm medical punch. Surface of PDMS and slide glass were treated by using plasma equipment (Cute-MP; Femto Science, Korea) and attach each other. AS-NCNM (anion selective-nanochannel network membrane) and CS-NCNM (cation selective-nanochannel network membrane) were fabricated by the self-assembly of  $\text{NR}_3^+$  functionalized nanoparticles (Micromod, Germany) and  $\text{COOH}^-$  functionalized nanoparticles (Micromod, Germany). The multi-layered bipolar ionic diode was developed by constructing AS-NCNM and CS-NCNM at the designed region in the multi-layered microchannels. As shown in Figure 1B, ethanol 70% was injected through reservoir in deep channel A, ethanol was stopped at the boundary between shallow channel and deep channel B by neck pressure [28]. Following, a diluted nanoparticles (surface:  $\text{NR}_3^+$ , Diameter: 200nm) were injected in deep channel and the nanoparticle moved to shallow [29]. When the nanoparticles are filled in the desired region and the diluted nanoparticles were removed, AS-NCNM was completed. After diluted nanoparticle injection (surface:  $\text{COOH}^-$ , diameter:100 nm) in the deep channel A, the nanoparticles were fully filled with shallow channel, and then the diluted nanoparticles were removed, and CS-NCNM was completed. The finished device was dried for one day and then used for the experiment.

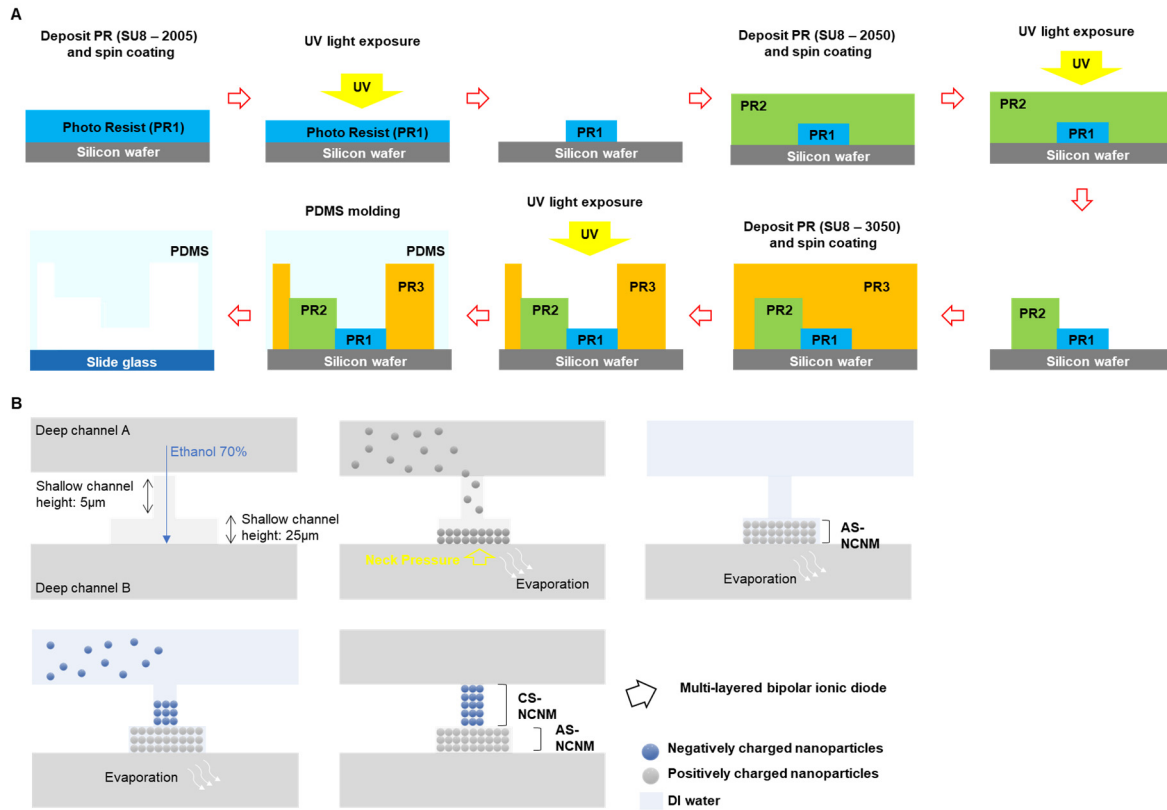


**Figure 1.** Fabrication of multi-layered bipolar ionic diode (A) Soft-lithography process to fabricate double layers bipolar ionic diode by using negative photoresist. (SU-8 2005: target 5 $\mu$ m height, SU-8 2050: target 25 $\mu$ m height, and SU-8 3050: target 100 $\mu$ m height. (B) Fabrication process for CS-NCNM and AS-NCNM by using self-assembly of nanoparticles.

## 2.2. Fabrication process for multi-layered bipolar ionic diode

Before the experiment nanopores of NCNMs were washed twice with 70% ethanol and then washed three times with DI water. Subsequently, the target concentration of KCl was injected, and ~30 min were waited for equilibrium to be reached. PT electrodes were connected into the reservoir of PDMS device, applying voltage to the tip and grounding the base. Ion current was measured from -9V to 9 V (interval 0.2V per 1s) using a picoammeter (6487, Keithley).

## 2.3. Numerical modeling for simulation

Modeling for the simulation of single- and multi-layered was performed using the finite element method (COMSOL, Multiphysics 5.6). The physics for the two-dimensional model used "Transport of Diluted Species" and "Electrostatics", which were solved by Nernst Planck equation and Poisson's equation respectively [27,30]. First electric potential is solved by equation (1):

$$\nabla^2 \varphi = -\frac{F}{\epsilon_0 \epsilon_r} \sum z_i c_i \quad (1)$$

where  $\varphi$ ,  $F$ , and  $z$  are the electrical potential, Faraday constant, and valence respectively. And  $c$ ,  $\epsilon_0$ , and  $\epsilon_r$  are ion concentration of ion species  $i$ , the vacuum permittivity, and the dielectric constant of the electrolyte solution. Following, the transport of potassium and chloride ions is solved by Nernst-Planck equation (2):

$$j_i = D_i + \frac{F z_i c_i}{RT} \nabla \varphi \quad (2)$$

And the continuity equation (3):

$$\nabla \cdot j_i = 0 \quad (3)$$

where  $D$  and  $j$  are coefficients of ions diffusion and ion flux of ion species  $i$ , respectively.  $R$  and  $T$  are constant of the gas universal and solution temperature.

Simulation model was drawn with the same size as the real bipolar ionic device and set the height using the out-of-plane thickness setting in the electrostatic module. For potential  $\varphi$ , boundary conditions are governed by the Gauss law (4):

$$-\bar{n} \cdot \nabla \varphi = \frac{\sigma}{\varepsilon_0 \varepsilon_r} \quad (4)$$

where  $\sigma$  is the surface charge density.

The surface charge density in the deep channel is used by equation (5):

$$\rho_{\text{deep}} = F(z_{\text{cation}}c_{\text{cation}} + z_{\text{anion}}c_{\text{anion}}) \quad (5)$$

where  $z_{\text{cation}}$  and  $z_{\text{anion}}$  are the charge numbers of cation and anion,  $c_{\text{cation}}$ ,  $c_{\text{anion}}$  are ion concentration of cation and anion respectively. The surface charge density in the shallow channel is used by equation (6) with the  $z_{\text{membrane}}$   $c_{\text{membrane}}$  term as an assumption for the membrane on which nanoparticles are assembled.

$$\rho_{\text{shallow}} = F(z_{\text{cation}}c_{\text{cation}} + z_{\text{anion}}c_{\text{anion}} + z_{\text{membrane}}c_{\text{membrane}}) \quad (6)$$

where  $z_{\text{membrane}}$  and  $c_{\text{membrane}}$  are the charge number of membrane surface and concentration of membrane.  $c_{\text{membrane}}$  is calculated by equation (7):

$$c_{\text{membrane}} = \frac{4\pi r^2 n \sigma}{e N_A (1 - 0.74)V} \quad (7)$$

where  $\sigma$  is the surface charge density of silica nanoparticles,  $n$  is total number of nanoparticles in NCNM ( $n = 3/4 \times 0.74 \times V/(\pi r^3)$ ) [27,30], and  $r$ ,  $e$ , and  $N_A$  are nanoparticles radius, the electron charge, and Avogadro's number, respectively.

### 3. Results and discussion

#### 3.1. Working principle of multi-layered bipolar ionic diode based on NCNM

Figure 2A shows a schematic of multi-layered bipolar ionic diode based on NCNM with ion distributions due to its polarized surface charge and asymmetric geometry. Figure 2B depicts the image of inverted microscope of the bipolar diode according to the proposed fabrication process. Figure 2C shows the ionic transport and distributions rely on the applied potential. The bipolar diode has the preferred ionic distributions in terms of surface charge polarity. A heterogeneous ionic junction, analogous to a p-n junction in a solid-state diode device, forms at the interface of two oppositely charged surfaces. The ions are in equilibrium without potential bias: cations are in CS-NCNM, and anions are in AS-NCNM due to electrostatic interaction between ions and surface charge. When a forward bias is applied, an accumulation region near the heterogeneous junction forms in which both ions are concentrated, and potential gradients along the NCNM drive high transport of ions. When the bias is reversed, a depletion region forms at the junction, and ion transport is suppressed.



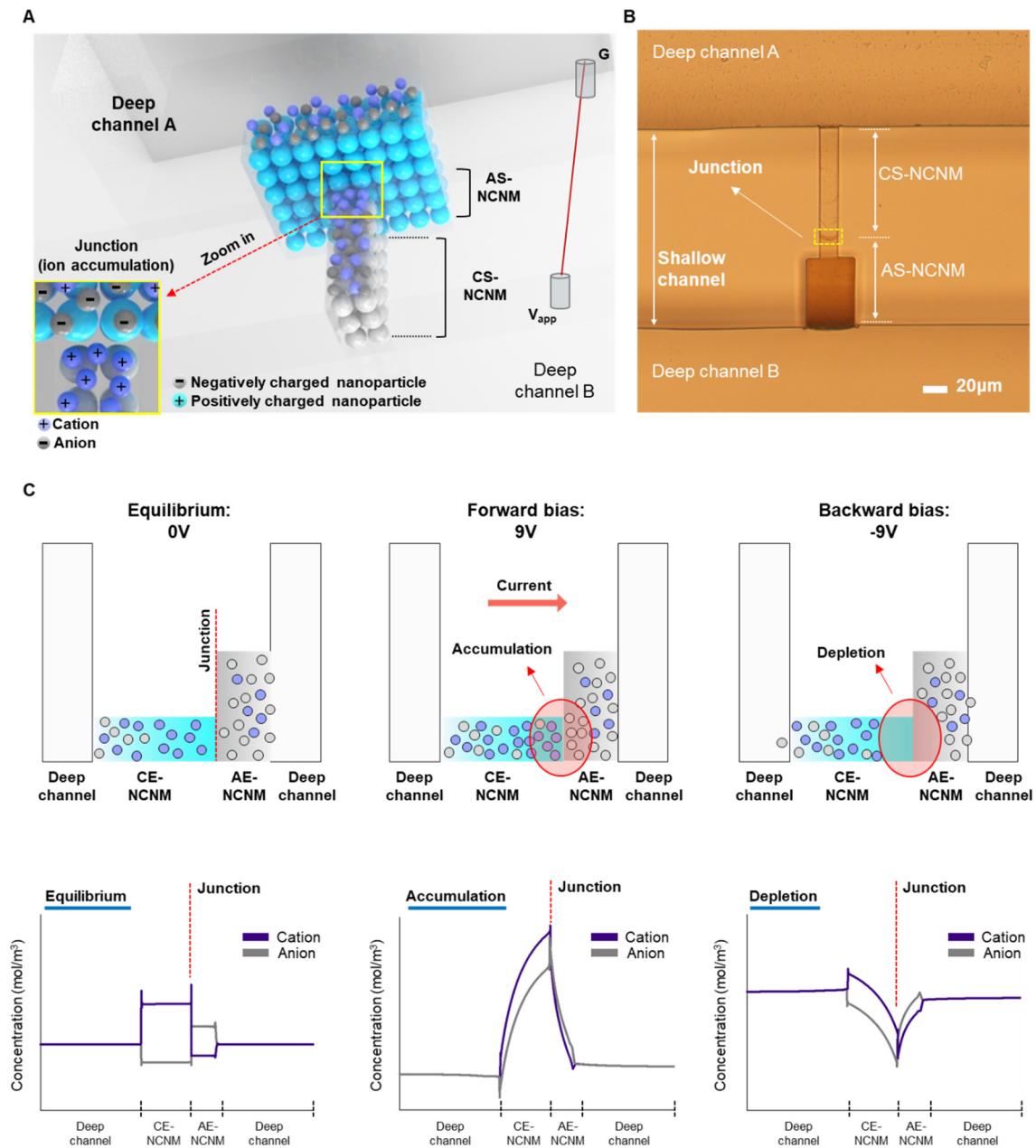


**Figure 2.** Schematic, fabrication result, and working principle of the proposed multi-layered bipolar ionic diode. (A) Schematic of multi-layered bipolar ionic diode (B) Microscopic image of the fabricated multi-layered bipolar ionic diode. (C) Working principle of multi-layered bipolar ionic diode that presents the different ionic distributions depending on the direction of the applied potential.

### 3.2. Characterization of ionic rectification according to the change of geometry

Ionic rectification was investigated with respect to the change of geometry in NCNMs experimentally. As shown in Figure 3A, the cuboid (width: 200  $\mu\text{m}$ , height: 100  $\mu\text{m}$ , length: 150  $\mu\text{m}$ ) are referred to as reference volumes, and the volume ratio of AS-NCNM and CS-NCNM to the reference volume is called ANR and CNR, respectively. The initial geometry parameters were based on the optimized geometry result from our previous work for a single-layered case [27], which has CS-NCNM filled with negatively charged particles (diameter: 100 nm, surface:  $\text{COOH}^-$ ) and AS-NCNM filled with positively charged particles (diameter: 200 nm, surface:  $\text{NR}_3^+$ ). From this, we increased the height of AS-NCNM from 5  $\mu\text{m}$  to 25  $\mu\text{m}$  and changed the width of AS-NCNM to 40  $\mu\text{m}$ , 100  $\mu\text{m}$ , and 200  $\mu\text{m}$ , respectively. The smaller the volume ratio of AS-NCNM under a KCl concentration of 10 mM, the higher the ICR. (ICR 154 at CNR: 0.0025, ANR: 0.0833, ICR 243 at CNR:

0.0025, ANR: 0.0417, ICR 367 at CNR: 0.0025, ANR: 0.0167). This result is supported by our previous result: The smaller area shows higher ion selectivity [31].

Following, we performed a similar investigation for observing the effect of the change in length of CS-NCNM and AS-NCNM (Figure 4A). Overall, the higher the total volume ratio of NCNM, the higher the ion current. The maximum ICR value was found when the CNR to ANR volume ratio was 0.0025:0.0167, and very surprisingly, the volume for AS-NCNM and CS-NCNM in the optimal geometry in the multilayered device was the same as the volumes for AS-NCNM and CS-NCNM in the single-layered device [27].

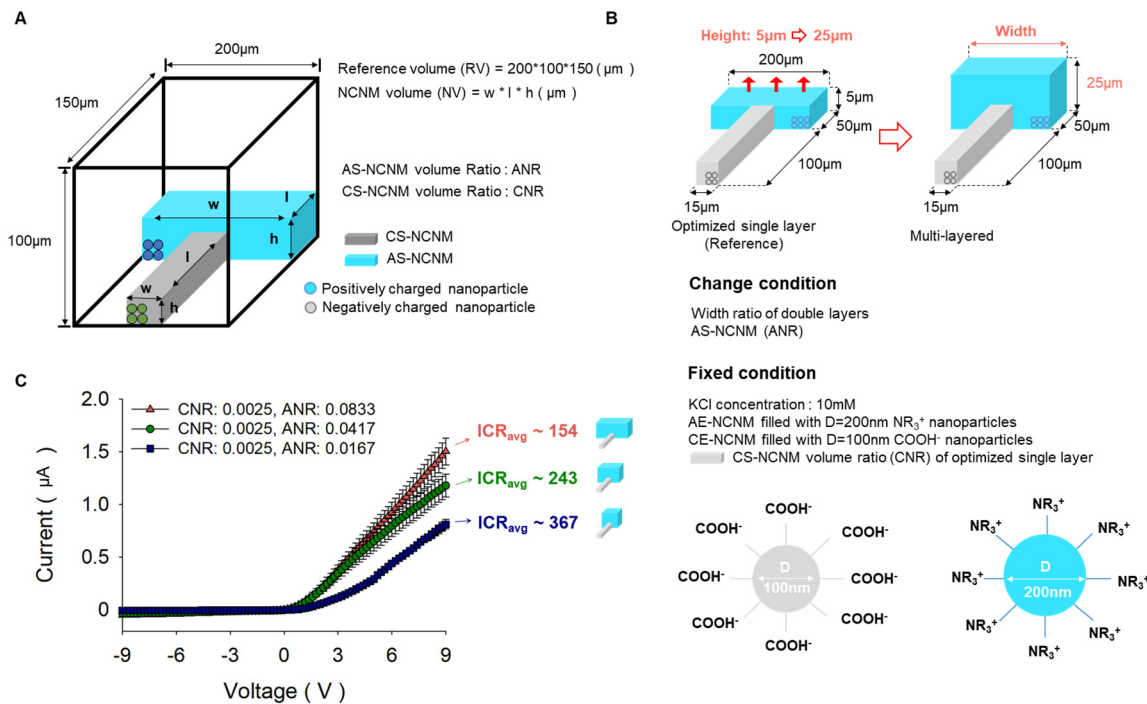


**Figure 3.** Investigation of the ICR value for multi-layered bipolar ionic diode according to the change of geometry (A) Definition of AS-NCNM and CS-NCNM volume ratio. (B) Experiment condition of nanoparticles, KCl concentration and geometry change for multi-layered bipolar ionic diode (C) I-V curve results for multi-layered bipolar ionic diode according to the change of width in AS-NCNM.

### 3.3. KCl concentration optimization of the multi-layered bipolar ionic diode

The ratio between the nanopore size and EDL thickness ( $R = d_n / \lambda_D$ ,  $\lambda_D$  and  $d_n$  are the EDL and nanopore size, respectively) is a critical factor for ion selectivity at NCNMs, and naturally, the factor  $R$  is also affected by the EDL thickness related with the ion concentration [31]. Therefore, an experiment was conducted to increase the ICR by adjusting the concentration of KCl to 0.1, 1, 3, 10, 100, and 400 mM. As a result, it was optimized at 3mM as  $\text{ICR} \sim 626$ . Especially in KCl 0.1mM and 100mM (Figure 4C), the ICR value of multi-layered bipolar ionic diode is respectively 1.5 times and 25 times better than single-layered bipolar ionic diode in the same concentration. As shown in numerical simulation results (Figure 5), when KCl 100mM was applied to a single-layered ionic diode, KCl was accumulated four times (400mM) for forward bias, but five times (500mM) for multi-layered. In addition, the ion depletion phenomena of multi-layered was slightly higher than that of single-layered in backward bias. In Figure 5c, the accumulation at 1 mM was 20 times in the single-layered and 40 times in the multi-layered, resulting in the multi-layered working better. In other words, the ionic rectification phenomenon of multi-layered was more prominent at higher and lower concentrations than that of single-layered. As shown in Table 1, many bipolar diodes, including our single-layered case, have a high rectification ratio in the specific salt concentration (though some cases have higher rectification than ours), but the proposed multi-layered device has stable rectification performance over a wide range of salt concentrations.

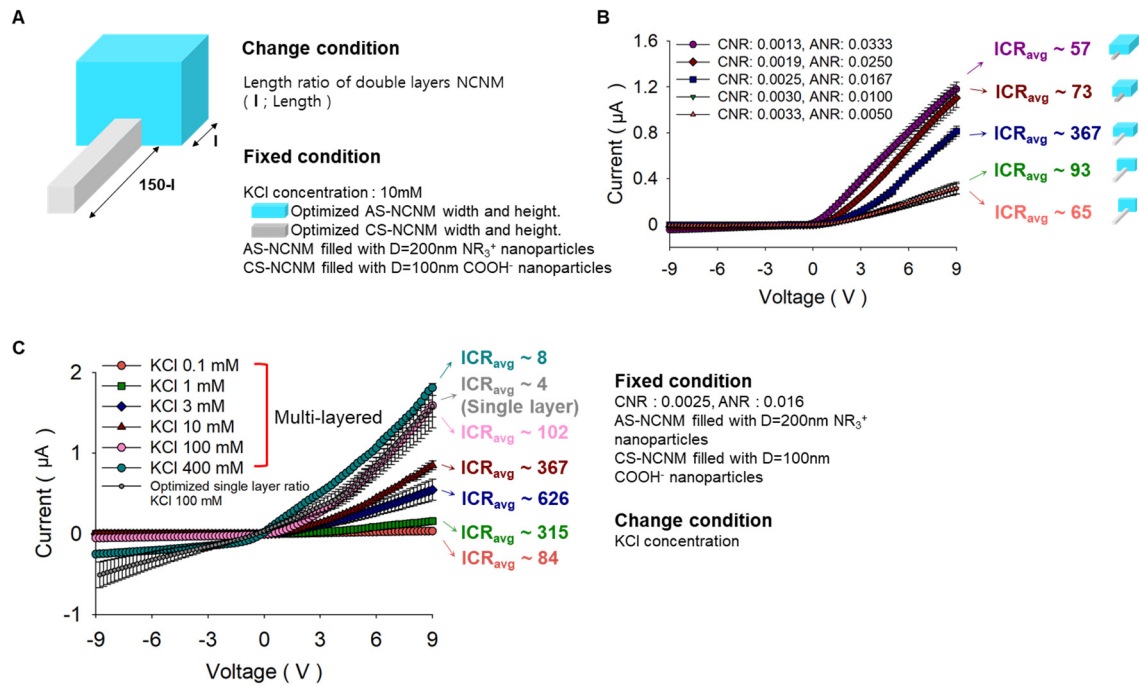


**Figure 4.** Exploration of ICR characteristics according to the change of length ratio and various salt concentrations. (A) Experiment conditions for KCl concentration, nanoparticles, and length ratio of AS-NCNM and CS-NCNM of the multi-layered bipolar ionic diode. (B) I-V curve of ICR results with respect to the length ratio of AS-NCNM and CS-NCNM of the multi-layered bipolar ionic diode. (C) I-V curve of ICR results for various KCl concentrations.

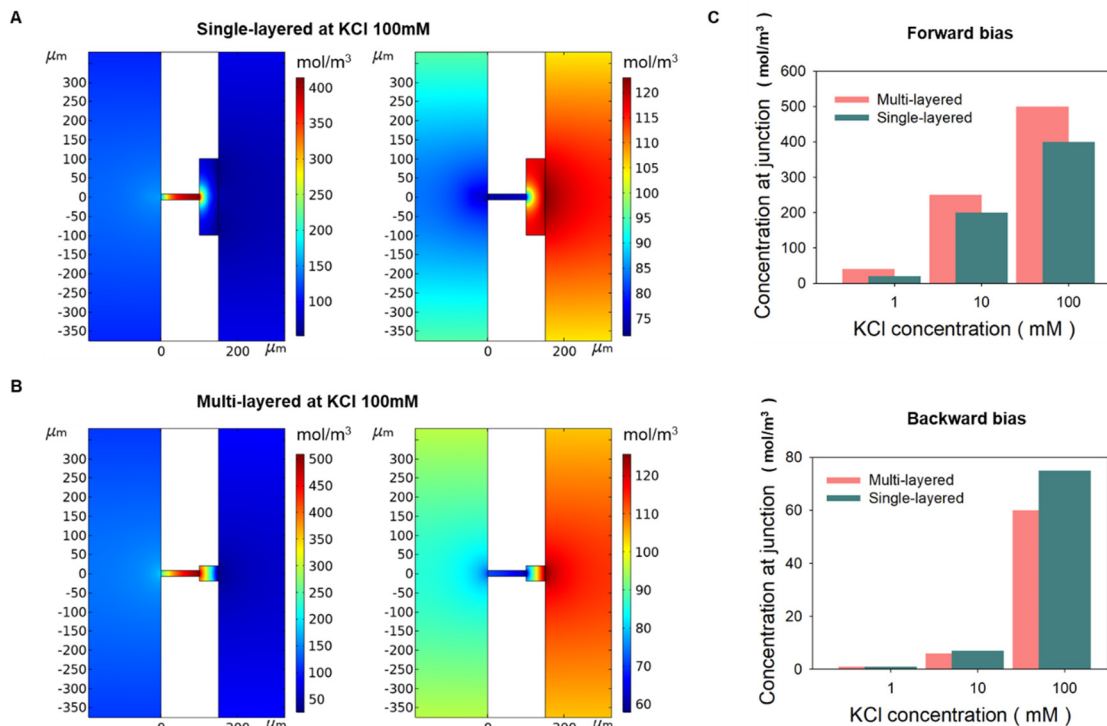


**Figure 5.** Numerical multi-physics simulation (A) When forward and backward bias was applied at KCl 100mM, concentration at junction on 2D single-layered simulation model. (B) When forward and backward bias was applied at KCl 100mM, concentration at junction on 2D multi-layered simulation model. (C) The concentration of forward bias and backward bias at junction when KCl 1, 10, 100mM.



**Table 1.** Comparison of ion current rectification of other works with proposed device in various ionic concentration.

Author, [ref] year	Material, device fabrication method	Voltage bias	ICR in 0.1mM and 1mM	10mM	100mM
Zhang et al., [12] 2015	Poly(ethylene terephthalate) (PET)/track etching technique	From -2 to 2V	0.1mM ~100 1mM ~430	~1000	~200
Li et al., [13] 2019	Polycarbonate (PC)/track etching technique	From -1 to 1V	0.1mM ~5 1mM ~7	~100	~650
Zhao et al., [14] 2020	Poly(ethylene terephthalate) (PET)/track etching technique	From -2 to 2V	1mM ~10	~200	~250
Liu et al., [15] 2020	Anodic aluminum oxide (AAO)/anodization	From -2 to 2V	0.1mM ~20 1mM ~80	~500	~100
Liu et al., [32] 2020	Polyacrylic acid (PAA)/anodization	From -1 to 1V	0.1mM ~300 1mM ~430	~160	~30
Kim et al., [27] 2022	Polydimethylsiloxane (PDMS)/soft lithography	From -9 to 9V	0.1mM ~50 1mM ~200	~370	~4
This study	Polydimethylsiloxane (PDMS)/soft lithography	From -9 to 9V	0.1mM ~85 1mM ~320	~370	~100

#### 4. Conclusions

We propose a multi-layered bipolar ionic diode made of AS- and CS-NCNM produced by nanoparticle self-assembly in this study. The geometry modification of NCNM and surface charge management is very simple and freely adjustable due to the relatively simple soft-lithography and functionalization, proper size, and material selection of nanoparticles. ICR features were explored with respect to changes in NCNM shape and ion concentration, and we discovered that the highest ICR in a multi-layered ionic diode was reached when each AS- and CS-NCNM volume was the same as each volume in a single-layered device (our previous result). The multi-layered diode exhibits stable ICR performance over a wide range of salt concentrations. Additionally, the outcomes of the numerical simulations show that the multi-layered bipolar ionic diode performs ion rectification better than the single-layered device in terms of overall salt concentration.

This characteristic is desirable for real-world applications since it means that bipolar diode-based devices, such as biosensors, desalination, and energy harvesting, can be used in a wide range of settings.

**Author Contributions:** J.K. designed and performed the experimental setup, device fabrication, materials and device characterizations, data analysis, Multiphysics simulation and manuscript writing. C.W. performed the device fabrication and characterization. J.P. led the project and participated in experimental design, data acquisition, and analysis, discussions, and manuscript writing. The manuscript was written based on the contributions of all the authors. All authors have read and agreed to the published version of the manuscript.

**Funding:** This work was supported by a National Research Foundation of Korea (NRF) grant funded by the Korean government (MSIP) (2020R1A2C2009093) and by the Korea Environment Industry & Technology Institute (KEITI) through its Ecological Imitation-based Environmental Pollution Management Technology Development Project funded by the Korea Ministry of Environment (MOE) (2019002790007).

**Data Availability Statement:** Data presented in this article are available on request from the corresponding author.

**Conflicts of Interest:** The authors declare no conflict of interest.

## References

- Choi, E.; Kwon, K.; Kim, D.; Park, J. Tunable reverse electrodialysis microplatform with geometrically controlled self-assembled nanoparticle network. *Lab Chip*. **2015**, *15*, 168-178
- Han., S. H.; Kwon., S.-R.; Baek., S.; Chung., T.-D. Ionic Circuits Powered by Reverse Electrodialysis for an Ultimate Iontronic System. *Scientific reports*. **2017**, *7*, 14068
- Cao, L.; Guo, W.; Ma, W.; Wang, L.; Xia, F.; Wang, S.; Wang, Y.; Jiangbc, L.; Zhub, D. Towards understanding the nanofluidic reverse electrodialysis system: well matched charge selectivity and ionic composition. *Energy & Environmental Science*. **2011**, *4*, 2259-2266
- Xiao, K.; Jiang, L.; Antonietti, M. Ion Transport in Nanofluidic Devices for Energy Harvesting. *Joule*. **2019**, *3*, 2364-2380
- Guo, W.; Cao, L.; Xia, J.; Nie, F.-Q.; Ma, W.; Xue, J.; Song, Y.; Zhu, D.; Wang, Y.; Jiang., L. Energy Harvesting with Single-Ion Selective Nanopores: A Concentration Gradient-Driven Nanofluidic Power Source. *Advanced functional materials*. **2010**, *20*, 1339-1344
- Choi,, C. W. E.; Park,, J. High-voltage nanofluidic energy generator based on ion-concentration-gradients mimicking electric eels. *Nano Energy*. **2018**, *43*, 291-299
- Xie, B.; Xiong, T.; Li, W.; Gao, T.; Zong, J.; Liu, Y.; Yu., P. Perspective on Nanofluidic Memristors: From Mechanism to Application. *Chemistry an asian journal*. **2022**, *17*, e202200682
- XIONG, T.; LI, C.; HE, X.; XIE, O.; ZONG, S.; JIANG, Y.; MA, W.; WU, F.; FEI, J.; YU, P.; MAO, L. Neuromorphic functions with a polyelectrolyte-confined fluidic memristor. *Science*. **2023**, *379*, 156-161
- Wang, Y.; Zhang, Z.; Xu, M.; Yang, Y.; Ma, M.; Li, H.; Pei, J.; Shi, L. Self-Doping Memristors with Equivalently Synaptic Ion Dynamics for Neuromorphic Computing. *ACS Appl Mater Interfaces*. **2019**, *11*, 24230-24240
- Wei, C.; Bard, A. J.; W., S.; Feldberg. Current Rectification at Quartz Nanopipet Electrodes. *Analytical chemistry*. **1997**, *69*, 4627-4633
- Nguyen, G.; Vlassioux, I.; Siwy, Z. S. Comparison of bipolar and unipolar ionic diodes. *Nanotechnology*. **2010**, *21*, 265301
- Zhang, Z.; Kong, X.-Y.; Xiao, K.; Liu, Q.; Xie, G.; Li, P.; Ma, J.; Tian, Y.; Wen, L.; Jiang, L. Engineered Asymmetric Heterogeneous Membrane: A Concentration-Gradient-Driven Energy Harvesting Device. *Journal of the American Chemical Society*. **2015**, *137*, 14765-14772
- Li, Z.-Q.; Wang, Y.; Wu, Z.-Q.; Wu, M.-Y.; Xia, X.-H. Bioinspired Multivalent Ion Responsive Nanopore with Ultrahigh Ion Current Rectification. *The Journal of Physical Chemistry C*. **2019**, *123*, 13687-13692
- Zhao, C.; Zhang, H.; Hou, J.; Ou, R.; Zhu, Y.; Li, X.; Jiang, L.; Wang, H. Effect of Anion Species on Ion Current Rectification Properties of Positively Charged Nanochannels. *ACS Applied Materials & Interfaces*. **2020**, *12*, 28915-28922
- Liu, Q.; Liu, Y.; Lu, B.; Wang, Y.; Xu, Y.; Zhai, J.; Fan, X. A high rectification ratio nanofluidic diode induced by an "ion pool". *RSC Advances*. **2020**, *10*, 7377-7383
- Liu, F. F.; Guo, Y. C.; Wang, W.; Chen, Y. M.; Wang, C. In situ synthesis of a MOFs/PAA hybrid with ultrahigh ionic current rectification. *Nanoscale*. **2020**, *12*, 11899-11907
- Cervera, J.; Schiedt, B.; Neumann, R.; Mafé, S.; Ramírez, P. Ionic conduction, rectification, and selectivity in single conical nanopores. *The journal of Chemical Physics*. **2006**, *124*, 104706
- Ma, T.; Gaigalas, P.; Lepoitevin, M.; Plikusiene, I.; Bechelany, M.; Janot, J.-M.; Balanzat, E.; Balme, S. Impact of Polyelectrolyte Multilayers on the Ionic Current Rectification of Conical Nanopores. *Langmuir*. **2018**, *34*, 3405-3412
- Cao, L.; Guo, W.; Wang, Y.; Jiang, L. Concentration-gradient-dependent ion current rectification in charged conical nanopores. *Langmuir*. **2012**, *28*, 2194-2199
- Lin, L.; Yan, J.; Li, J. Small-molecule triggered cascade enzymatic catalysis in hour-glass shaped nanochannel reactor for glucose monitoring. *Analytical chemistry*. **2014**, *86*, 10546-10551
- Hou, S.; Wang, Q.; Fan, X.; Liu, Z.; Zhai, J. Alumina Membrane with Hour-Glass Shaped Nanochannels: Tunable Ionic Current Rectification Device Modulated by Ions Gradient. *Journal of Nanomaterials*. **2014**, *2014*, 1-10
- Wang, Y.; Wang, Z.; Su, Z.; Cai, S. Stretchable and transparent ionic diode and logic gates. *Extreme Mechanics Letters*. **2019**, *28*, 81-86

23. Xiao, K.; Xie, G.; Zhang, Z.; Kong, X.-Y.; Qian Liu, P. L.; Wen, L.; Jiang, L. Enhanced Stability and Controllability of an Ionic Diode Based on Funnel-Shaped Nanochannels with an Extended Critical Region. *Advanced Materials*. **2016**, 28, 3345-3350
24. Nguyen, Q. H.; Ali, M.; Nasir, S.; Ensinger, W. Transport properties of track-etched membranes having variable effective pore-lengths. *Nanotechnology*. **2015**, 26, 485502
25. Ali, M.; Ramirez, P.; Nasir, S.; Nguyen, Q.-H.; Ensinger, W.; Mafe, S. Current rectification by nanoparticle blocking in single cylindrical nanopores. *Nanoscale*. **2014**, 6, 10740-10745
26. Pu, Q.; Yun, J.; Temkin, H.; Liu, S. Ion-Enrichment and Ion-Depletion Effect of Nanochannel Structures. *Nano letters*. **2004**, 4, 1099-1103
27. Kim, J.; Jeon, J.; Wang, C.; Chang, G. T.; Park, J. Asymmetric Nanochannel Network-Based Bipolar Ionic Diode for Enhanced Heavy Metal Ion Detection. *ACS Nano*. **2022**, 16, 8253-8263
28. Cho, H.; Kim, H.-Y.; Kang, J. Y.; Kim, T. S. How the capillary burst microvalve works. *Journal of Colloid and Interface Science*. **2007**, 306, 379-385
29. Chung, S.; Yun, H.; Kamm, R. D. Nanointerstice-driven microflow. *Small*. **2009**, 5, 609-613
30. Choi, E.; Wang, C.; Chang, G. T.; Park, J. High Current Ionic Diode Using Homogeneously Charged Asymmetric Nanochannel Network Membrane. *Nano Lett*. **2016**, 16, 2189-2197
31. Choi, E.; Wang, C.; Chang, G. T.; Park, J. High Current Ionic Diode Using Homogeneously Charged Asymmetric Nanochannel Network Membrane. *Nano Letters*. **2016**, 16, 2189-2197
32. Liu, F.-F.; Guo, Y.-C.; Wang, W.; Chen, Y.-M.; Wang, C. In situ synthesis of a MOFs/PAA hybrid with ultrahigh ionic current rectification. *Nanoscale*. **2020**, 12, 11899-11907

**Disclaimer/Publisher's Note:** The statements, opinions and data contained in all publications are solely those of the individual author(s) and contributor(s) and not of MDPI and/or the editor(s). MDPI and/or the editor(s) disclaim responsibility for any injury to people or property resulting from any ideas, methods, instructions or products referred to in the content.